Journal of Power Sources 188 (2009) 313–318

Contents lists available at ScienceDirect

Journal of Power Sources

journal homepage: www.elsevier.com/locate/jpowsour

Short communication

A high-performance counter electrode based on poly(3,4-alkylenedioxythiophene) for dye-sensitized solar cells☆

Kun-Mu Lee[a], Po-Yen Chen[b], Chih-Yu Hsu[b], Jen-Hsien Huang[b], Wen-Hsien Ho[c], Hung-Chang Chen[c], Kuo-Chuan Ho[a,b,*]

[a] Institute of Polymer Science and Engineering, National Taiwan University, Taipei 10617, Taiwan
[b] Department of Chemical Engineering, National Taiwan University, Taipei 10617, Taiwan
[c] Department of Product Development, Taiwan Textile Research Institute, Tucheng 23674, Taiwan

ARTICLE INFO

Article history:
Received 9 September 2008
Received in revised form
18 November 2008
Accepted 19 November 2008
Available online 28 November 2008

Keywords:
Conducting polymer
Dye-sensitized solar cells
Counter electrode
PProDOT-Et_2

ABSTRACT

A poly(3,3-diethyl-3,4-dihydro-2H-thieno-[3,4-b][1,4]dioxepine) (PProDOT-Et_2) counter electrode prepared by electrochemical polymerization on a fluorine-doped tin oxide (FTO) glass substrate was incorporated in a platinum-free dye-sensitized solar cell (DSSC). The surface roughness and I^-/I_3^- redox reaction behaviors based on PProDOT-Et_2, poly(3,4-propylenedioxythiophene) (PProDOT), poly(3,4-ethylenedioxythiophene) (PEDOT), and sputtered-Pt electrodes were characterized, and their performances as counter electrodes in DSSCs were compared. Cells fabricated with a PProDOT-Et_2 counter electrode showed a higher conversion efficiency of 7.88% compared to cells fabricated with PEDOT (3.93%), PProDOT (7.08%), and sputtered-Pt (7.77%) electrodes. This enhancement was attributed to increases in the effective surface area and good catalytic properties for I_3^- reduction. In terms of the film thickness effect, the fill factor was strongly dependent on the deposition charge capacity of the PProDOT-Et_2 layer, but the aggregation of PProDOT-Et_2 in thicker layers (>80 mC cm^{-2}) resulted in decreases in J_{SC} and the cell conversion efficiency. The charge transfer resistances (R_{ct1}) of the PProDOT-Et_2 counter electrodes had the lowest value of ~18 Ω at a deposition charge capacity of 40 mC cm^{-2}. These results indicate that films with high conductivity, high active surface area, and good catalytic properties for I_3^- reduction can potentially be used as the counter electrode in a high-performance DSSC.

1. Introduction

In 1991, the successful demonstration of dye-sensitized solar cells (DSSCs) introduced a novel approach to traditional inorganic silicon solar cells [1]. In order to further improve the performance of DSSCs, extensive research has been conducted on each constituent of the solar cells such as semiconductor nano-crystalline TiO_2 [2], dye molecules [3], electrolytes [4], and counter electrodes [5–7]. For the counter electrodes, although Pt has high catalytic activity for I_3^- reduction, high conductivity, and stability, it is one of the most expensive components in DSSCs. Therefore, development of counter electrodes with alternative materials is expected to reduce production costs of DSSCs. Several varieties of carbonaceous materials such as carbon nanotubes, activated carbon, graphite, and carbon black have been employed as catalysts for counter electrodes in DSSCs [7,8]. However, the internal resistance of a device increases with the thickness of the counter electrodes, resulting in a low fill factor and efficiency. Recently, Murakami et al. employed carbon black as the counter electrode in DSSCs and achieved a remarkable conversion efficiency of 9.1% under 100 mW cm^{-2} [7].

Meanwhile, Saito et al. used chemically polymerized poly(3,4-ethylenedioxythiophene) (PEDOT) on fluorine-doped tin oxide (FTO) glass as the counter electrodes and obtained a conversion efficiency of ~3.6% under 100 mW cm^{-2} [6]. Yanagida and co-workers also developed PEDOT-based solid-state electrolytes, but the cell efficiencies were <1% [9,10]. Considering the vast literature published on various components of DSSCs, it was found that only a few publications employed conducting polymers as counter electrodes, and few reports on electrochemical preparation exist.

Previously, we reported a counter electrode prepared by spin-coating poly(3,4-ethylenedioxythiophene):polystyrenesulphonate (PEDOT:PSS) containing carbon black and showed a comparable cell efficiency with cells using Pt electrodes [11]. In this paper, we report the properties of several poly(3,4-alkylenedioxythiophene)-derived films prepared by electrochemical polymerization which were used as counter electrodes for DSSCs. The influences of film morphologies, material conformations, and electrode-

☆ Presented at the 2nd International Conference on Functional Materials and Devices 2008, Kuala Lumpur, Malaysia, 16–19 June 2008.

* Corresponding author at: Department of Chemical Engineering, National Taiwan University, Taipei 10617, Taiwan. Tel.: +886 2 2366 0739; fax: +886 2 2362 3040.
E-mail address: kcho@ntu.edu.tw (K.-C. Ho).

0378-7753/$ – see front matter © 2008 Elsevier B.V. All rights reserved.
doi:10.1016/j.jpowsour.2008.11.075

position capacities on the performances of the DSSCs were investigated.

2. Experimental procedures

2.1. Materials

Anhydrous LiI, I_2, poly(ethylene glycol) (PEG) (MW 20,000), 4-tertiary butyl pyridine (TBP), tertiary butanol, and acetonitrile were purchased from Merck. 3,3-diethyl-3,4-dihydro-2H-thieno-[3,4-b][1,4]dioxepine (ProDOT-Et_2), 3,4-propylenedioxythiophene (ProDOT), 3,4-ethylenedioxythiophene (EDOT) were purchased from Aldrich. Titanium (IV) tetraisopropoxide (>98%) was purchased from Acros and used as received. N_3 dye (*cis*-di(thiocyanato)bis(2,2′-bipyridyl-4,4′-dicarboxylate)ruthenium (II)) was obtained from Solaronix (Aubonne, Switzerland).

2.2. Preparation of counter electrodes and TiO_2 electrodes

The conducting polymer films were electrodeposited onto FTO glass (R_{sh} = 15 Ω square^{-1}) by applying a constant potential of 1.1 V (vs. Ag/Ag$^+$) until the expected charge capacities were reached, and the Pt (100 nm thick) was sputtered onto the FTO glass. The structural nature was investigated using scanning electron microscopy (SEM, Hitachi S-4700) and atomic force microscopy (AFM, Digital Instruments, Dimension-3100 Multimode).

The TiO_2 nanoparticle preparation and electrode fabrication were carried out according to the literature [12] except after autoclave treatment, where the solution was concentrated to 13 wt.% and PEG was added to prevent film cracking during drying. The TiO_2 paste was coated onto FTO glass using a glass rod, and then sintered at 500 °C for 30 min.

2.3. Cell assembly and measurements of the DSSCs

An active area of 0.25 cm^2 was selected from the sintered TiO_2 electrode and immersed in a 3×10^{-4} M solution of N_3 dye containing acetonitrile and tertiary butanol (in a volume ratio of 1:1) overnight. The cell was assembled with the two electrodes separated by the electrolyte composed of 0.5 M LiI/0.05 M I_2/0.5 M TBP in acetonitrile and an ionomer resin of 50 μm (Surlyn 1702, Dupont).

The DSSCs were energized using a light source of a 450-W Xe lamp (#6266, Oriel) equipped with a water-based infrared (IR) filter and an AM 1.5 filter (#81075, Oriel). Photoelectrochemical characteristics and electrochemical impedance spectroscopic (EIS) measurements of the DSSCs were recorded with a potentiostat/galvanostat (PGSTAT 30, Autolab, Eco-Chemie) under constant light illumination of 100 mW cm^{-2}. The applied bias voltage was set at an open-circuit voltage of the DSSCs, and the AC amplitude was 10 mV between the counter and working electrodes, in the frequency range of 10 mHz to 65 kHz. The impedance spectra were analyzed based on an equivalent circuit model [13].

3. Results and discussion

3.1. Characterization of different conducting polymer films and the influence of the deposition charge capacity on the conformation and catalyst effects

Different conducting polymer films (PEDOT, PProDOT and PProDOT-Et_2), electropolymerized at a constant potential of 1.1 V (vs. Ag/Ag$^+$) on the FTO glass with a deposition charge capacity of 40 mC cm^{-2}, were characterized. The order of the root-mean-square (RMS) roughness, R_{rms}, was PProDOT-Et_2 > PProDOT > PEDOT > sputtered-Pt, as measured by AFM. The PProDOT-Et_2 film showed a wire-like and highly porous structure

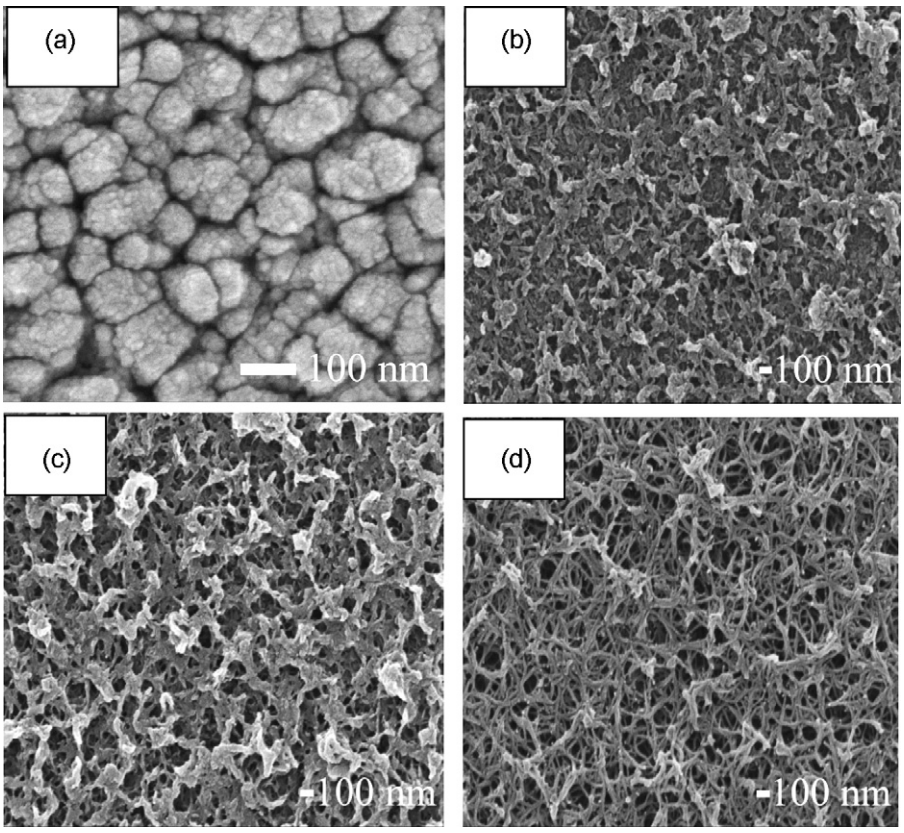

Fig. 1. The top view SEM images of various thin film materials: (a) Pt (100 nm), (b) PEDOT (40 mC cm^{-2}), (c) PProDOT (40 mC cm^{-2}), and (d) PProDOT-Et_2 (40 mC cm^{-2}).

Table 1
Cell performances of dye-sensitized solar cells (DSSCs) based on different kinds of counter electrode materials. These cell performances were measured under illumination at 100 mW cm^{-2}.

Counter electrode[a]	R_{rms}[b] (nm)	J_{LIM}[c] (mA cm^{-2})	V_{OC} (mV)	J_{SC} (mA cm^{-2})	η (%)	FF
Sputtered-Pt	23.6 ± 1.7	0.68 ± 0.04	715 ± 5	17.28 ± 0.40	7.77 ± 0.12	0.63 ± 0.01
PEDOT	53.7 ± 2.7	0.25 ± 0.02	705 ± 5	8.84 ± 0.50	3.93 ± 0.14	0.63 ± 0.01
PProDOT	61.3 ± 3.1	0.63 ± 0.05	715 ± 5	16.80 ± 0.60	7.08 ± 0.12	0.59 ± 0.01
PProDOT-Et$_2$	83.5 ± 2.2	0.67 ± 0.05	720 ± 5	18.00 ± 0.50	7.88 ± 0.10	0.61 ± 0.01

[a] The thickness of sputtered-Pt electrode was *ca.* 100 nm, and the PEDOT, PProDOT and PProDOT-Et$_2$ films were all electrodeposited at 40 mC cm^{-2} at a constant potential of 1.1 V (vs. Ag/Ag$^+$).
[b] R_{rms} means the root-mean-square roughness.
[c] The limiting current density (J_{LIM}) of various materials as working electrodes was measured in a three-electrode electrochemical cell.

due to the steric effect (refer to Fig. 1), so it was rougher than the PProDOT and PEDOT films. R_{rms} values of those films, which reflect the degree of surface roughness, are listed in Table 1. The PProDOT-Et$_2$ film showed the largest R_{rms} value of *ca.* 82 nm over a 5 × 5-μm area, indicating that the film possessed the largest surface area among those films. The limiting current densities (J_{LIM}) of different electrodes measured by chronoamperometry are also listed in Table 1. Although, the sputtered-Pt film had a lower value of R_{rms}, the high conductivity and good catalytic performance for reduction of I_3^-, leading to a high J_{LIM}, were as good as those of the PProDOT-Et$_2$ film. The high surface area arising from the wire-like nanoporous nature of the PProDOT-Et$_2$ film is advantageous for DSSC performance, which in turn enhances values of J_{SC}.

Cyclic voltammetry (CV) which analyzes the relationship between ion diffusivity and reaction kinetics of an electrochemical system was applied to the different electrodes as shown in Fig. 2. The two anodic and cathodic peaks represent the following reactions:

$$3I^- \leftrightarrow I_3^- + 2e^- \quad (1)$$

$$2I_3^- \leftrightarrow 3I_2 + 2e^- \quad (2)$$

Fig. 2 reveals larger anodic and cathodic peaks and associated charges for the PProDOT-Et$_2$ film than for the PProDOT and PEDOT films. Fig. 3a shows the CV of I^-/I_3^- redox couples on PProDOT-Et$_2$ film with various scan rates in acetonitrile, and the relationship between the anodic and cathodic peaks and square root of the scan rate is shown in Fig. 3b. The linear relationship indicates the diffusion limitation of the redox reaction on PProDOT-Et$_2$ film. In comparison to the Pt electrode, the redox reaction at the PProDOT-Et$_2$ surface was little affected by the adsorption of iodide species under these conditions. This also suggests that no specific interaction between I^-/I_3^- and the PProDOT-Et$_2$ electrode occurred, as in the case of the Pt electrode [6,14].

The influence of the deposition charge capacity on the conformation of the PProDOT-Et$_2$ films was also investigated from the top view of the SEM images, as shown in Fig. 4. The PProDOT-Et$_2$ film showed a dense conformation at 10 mC cm^{-2}, and then a porous structure emerged with a further increase to 40 mC cm^{-2}. However, aggregation appeared when the deposition charge capacity exceeded 80 mC cm^{-2} with large pores contained in the films. The PProDOT-Et$_2$ film even peeled off when the charge capacity exceeded 200 mC cm^{-2}. Those appearances, aggregation, and the presence of large pores in the films reduced the catalytic activity for I_3^- reduction.

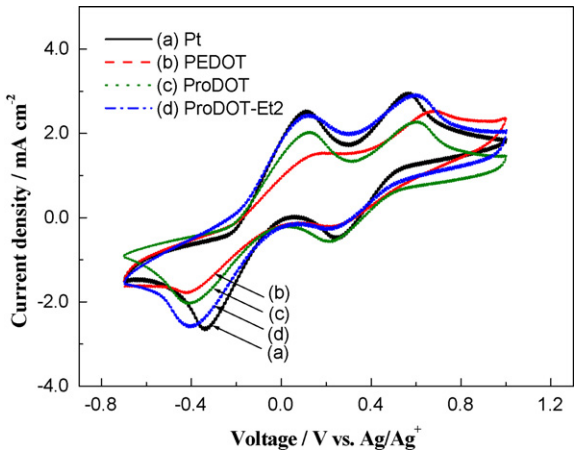

Fig. 2. Cyclic voltammetry (CV) of iodide species on different conducting polymer films and Pt electrodes in an acetonitrile solution with 10 mM LiI, 1 mM I_2, and 0.1 M $LiClO_4$.

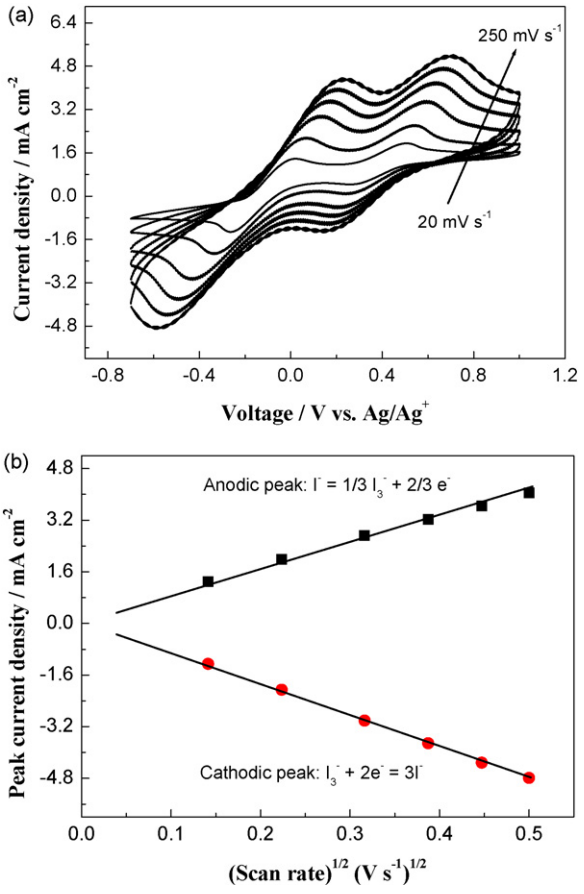

Fig. 3. (a) The CVs of iodide species on ProDOT-Et$_2$ film with various scan rates in acetonitrile solution of 10 mM LiI, 1 mM I_2 and 0.1 M $LiClO_4$ and (b) peak current as a function of scan rate in CV tests of (a).

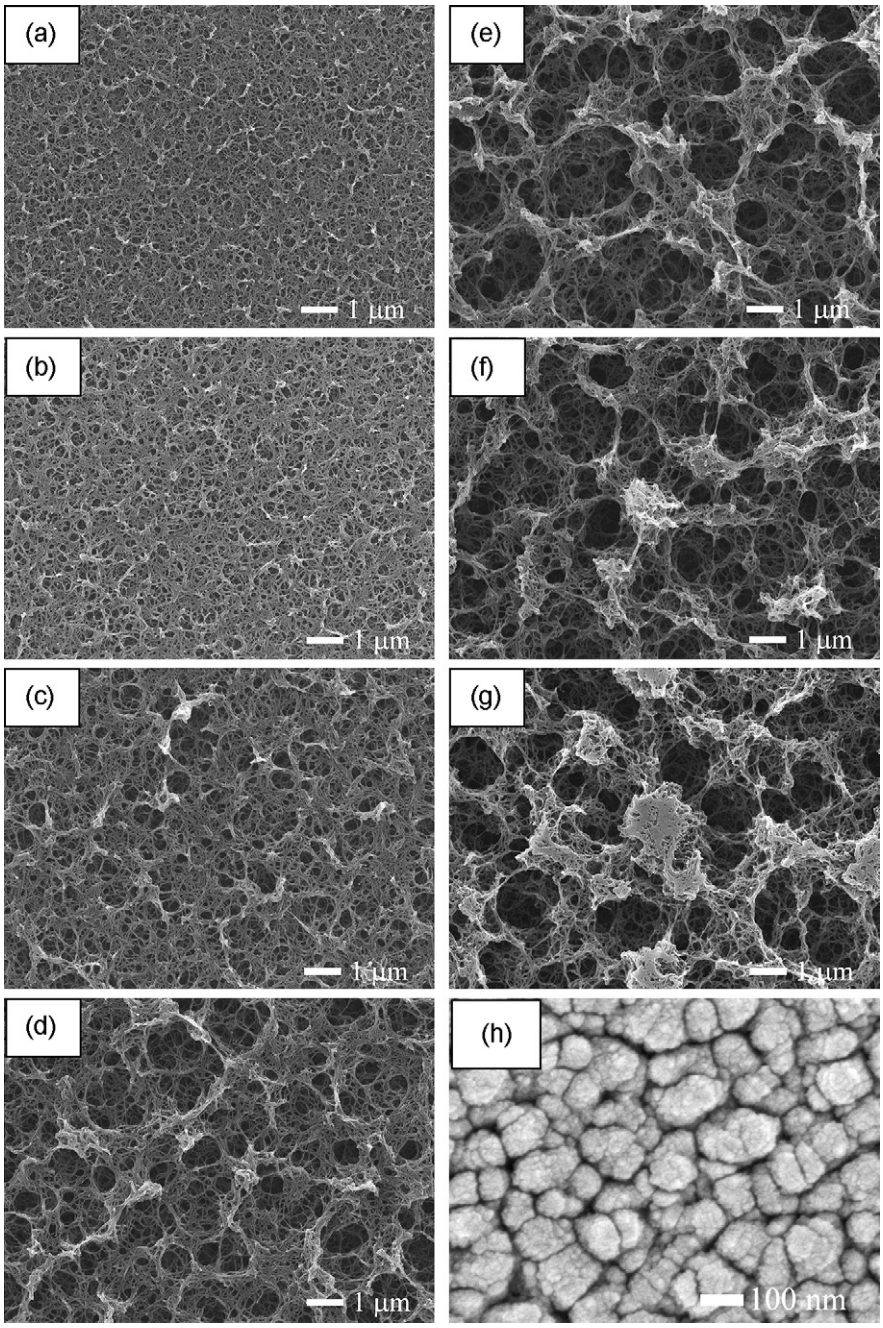

Fig. 4. SEM images of PProDOT-Et_2 films with various deposition charge capacities (×10,000): (a) 10 mC cm^{-2}, (b) 20 mC cm^{-2}, (c) 40 mC cm^{-2}, (d) 80 mC cm^{-2}, (e) 120 mC cm^{-2}, (f) 160 mC cm^{-2}, and (g) 200 mC cm^{-2}. (h) Image of sputtered-Pt (100 nm) for comparison.

3.2. Influences of the conducting polymer as the counter electrode and electrodeposition charge capacity on the performance of DSSCs

The photovoltaic parameters of DSSCs with different counter electrodes are given in Table 1. In fact, the PProDOT-Et_2 film revealed the highest active surface area, as judged by the root-mean-square roughness (R_{rms}). The DSSC with a PProDOT-Et_2 counter electrode had the highest short-circuit current density (J_{SC}) and open-circuit voltage (V_{OC}), and resulted in a good conversion efficiency of 7.88%, compared to 7.77% for the cell prepared with the sputtered-Pt electrode. The cell with the PEDOT counter electrode showed the lowest value of J_{SC} of 8.84 mA cm^{-2} due to its low active surface area. In addition, the incident photo-to-current conversion efficiency (IPCE) had the same trend (not shown here). The IPCE exceeded 70% in a spectral range from 400 to 560 nm and reached a maximum of about 80% at 520 nm for DSSCs with the sputtered-Pt and PProDOT-Et_2 counter electrodes. The value of IPCE for cells with the PProDOT electrode exhibited a small decrease; however, those with the PEDOT electrode only reached *ca.* 50% of the maximum value.

The photovoltaic performances with various deposition charge densities of PProDOT-Et_2 counter electrodes are shown in Fig. 5a, and the parameters are summarized in Fig. 5b and c. The V_{OC} of DSSCs was unaffected by changing the deposition charge capacity, and the average value was 0.72 ± 0.05 V (Fig. 5b). The most pronounced change was observed in the fill factor (FF), which significantly increased from 0.38 to 0.62 with an increase in the

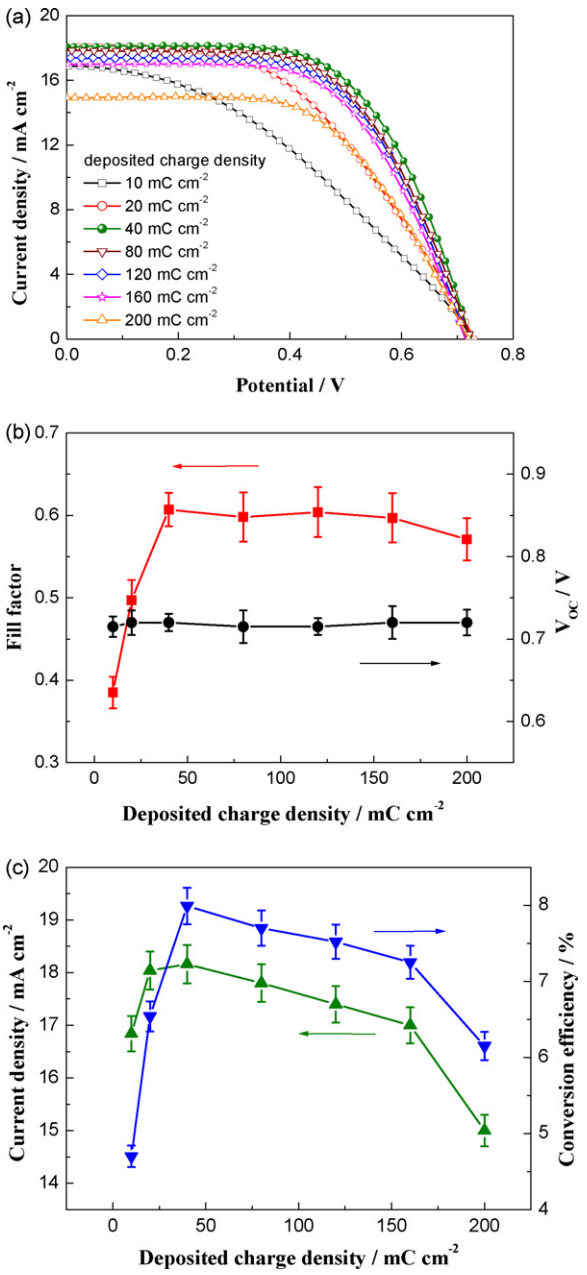

Fig. 5. (a) The *J*–*V* curve of dye-sensitized solar cells (DSSCs) based on PProDOT-Et_2 counter electrodes with different deposition charge capacities, and summarized in (b). The V_{OC} and FF of the DSSCs vs. the deposition charge capacity and (c) the J_{SC} and cell conversion efficiency of DSSCs vs. the deposition charge capacity.

deposition charge capacity of 10–40 mC cm^{-2}. At higher deposition charge capacities, values of FF remained around 0.62 (Fig. 5b). Fig. 5c reveals that the J_{SC} and cell conversion efficiency (η) increased from 16.8 to 18.2 mA cm^{-2} and from 4.6 to 7.9%, respectively, when the deposition charge capacity increased from 10 to 40 mC cm^{-2}. Further increases in the deposition charge capacity led to a decrease in the J_{SC} due to aggregation of PProDOT-Et_2 and the appearance of large pores in the film which reduced the active surface area. It is clear that the cells using bare FTO as the counter electrode with no catalyst performed poorly (only 0.02%) [7]. The necessity of depositing an effective catalyst onto the FTO counter electrode can easily be appreciated from the above results.

The EIS analysis of DSSCs with counter electrodes of various deposition charge capacities are shown in Fig. 6. Fig. 6a shows that the overall series resistances of the cell (R_S) decreased for

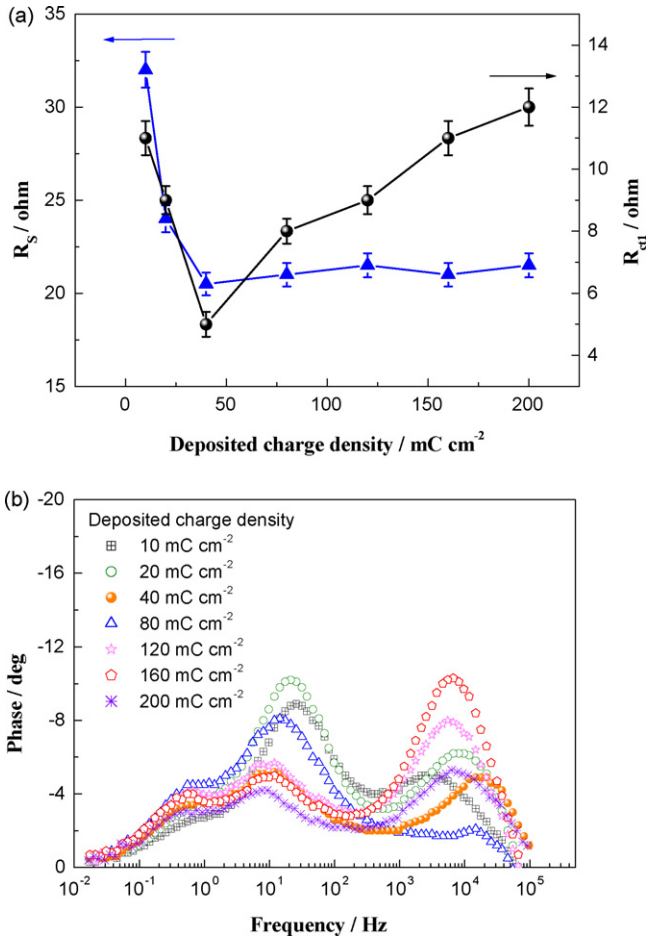

Fig. 6. EIS measurements of dye-sensitized solar cells (DSSCs). (a) The series resistance of the device (R_S) and the charge transfer resistance at the counter electrode/electrolyte interface (R_{ct1}) fitted from the Nyquist plots and (b) Bode phase plot.

deposition charge capacities of 10–40 mC cm^{-2}, indicating that the conductivity of the counter electrode increases with growth of the PProDOT-Et_2 film. The decrease in R_S improved the FF of the DSSCs to achieve better performance. As for the electrochemical reaction at the counter electrode interface in the high-frequency region (10^3–10^5 Hz), represented by R_{ct1}, it decreased from 11 to 5 Ω for deposition charge capacities of 10–40 mC cm^{-2} and further increased when the charge capacity exceeded 80 mC cm^{-2}. The lowest R_{ct1} value was noted at 40 mC cm^{-2}, due to the high active surface area and good catalytic property for the reduction of I_3^-. Furthermore, in the Bode phase plot (Fig. 6b), the characteristic peak value shifting to a higher frequency means that the redox reaction rate on the counter electrode is faster. It was found that the peak shifted to a higher frequency and then shifted back with an increase in the deposition charge capacity. The highest characteristic frequency peak was determined at a deposition charge capacity of 40 mC cm^{-2}. These EIS analyses also support the above photovoltaic results.

4. Conclusions

The effects of various conducting polymers as counter electrodes and the electrodeposition charge capacities on the performance of platinum-free DSSCs were studied. The PProDOT-Et_2-based DSSC showed the best cell performance, compared to that using PEDOT or PProDOT; this was due to the good catalytic property of PProDOT-Et_2 for reducing I_3^- and the higher surface active area from its

wire-like structure. The CV measurement involving the I^-/I_3^- redox reaction on the PProDOT-Et_2 electrode showed no major difference, compared to that of the sputtered-Pt electrode. The PProDOT-Et_2-based DSSC had the best conversion efficiency of 7.88% when the deposition charge capacity of PProDOT-Et_2 reached 40 mC cm^{-2}, with J_{SC}, V_{OC}, and FF values of 18.00 mA cm^{-2}, 0.72 V, and 0.61, respectively.

Acknowledgements

The authors appreciate the financial support provided by the National Science Council (NSC) of Taiwan, under grant numbers NSC 96-2120-M-002-016 and NSC 97-2120-M-002-012. This work was also partially supported by the Taiwan Textile Research Institute (TTRI), Tucheng City, Taipei County, Taiwan.

References

[1] B. O'Regan, M. Grätzel, Nature 353 (1991) 737–740.
[2] C.J. Barbe', F. Arendse, P. Comte, M. Jirousek, F. Lenzmann, V. Shklover, M. Grätzel, J. Am. Ceram. Soc. 80 (1997) 3157–3171.
[3] M.K. Nazeeruddin, P. Pechy, T. Renouard, S.M. Zakeeruddin, R. Humphry-Baker, P. Comte, P. Liska, C. Le, E. Costa, V. Shklover, L. Spiccia, G.B. Deacon, C.A. Bignozzi, M. Grätzel, J. Am. Chem. Soc. 123 (2001) 1613–1624.
[4] X. Zhang, H. Yang, H.M. Xiong, F.Y. Li, Y.Y. Xia, J. Power Sources 160 (2006) 1451–1455.
[5] C.H. Yoon, R. Vittal, J. Lee, W.S. Chae, K.J. Kim, Electrochim. Acta 53 (2008) 2890–2896.
[6] Y. Saito, W. Kubo, T. Kitamura, Y. Wada, S. Yanagida, J. Photochem. Photobiol. A: Chem. 164 (2004) 153–157.
[7] T.N. Murakami, S. Ito, Q. Wang, M.K. Nazeeruddin, T. Bessho, I. Cesar, P. Liska, R. Humphry-Baker, P. Comte, P. Pechy, M. Grätzel, J. Electrochem. Soc. 153 (2006) A2255–A2261.
[8] K. Suzuki, M. Yamamoto, M. Kumagai, S. Yanagida, Chem. Lett. 32 (2003) 28–29.
[9] N. Fukuri, Y. Saito, W. Kubo, G.K.R. Senadeera, T. Kitamura, Y. Wada, S. Yanagida, J. Electrochem. Soc. 151 (2004) A1745–A1748.
[10] R. Senadeera, N. Fukuri, Y. Saito, T. Kitamura, Y. Wada, S. Yanagida, Chem. Commun. (2005) 2259–2261.
[11] J.G. Chen, H.Y. Wei, K.C. Ho, Sol. Energy Mater. Sol. Cells 91 (2007) 1472–1477.
[12] M.K. Nazeeruddin, R. Humphry-Baker, P. Liska, M. Grätzel, J. Phys. Chem. B 107 (2003) 8981–8987.
[13] M.C. Bernard, H. Cachet, P. Falaras, A. Hugot-Le Goff, M. Kalbac, I. Lukes, N.T. Oanh, T. Stergiopoulos, I. Arabatzis, J. Electrochem. Soc. 150 (2003) E155–E164.
[14] A. Hauch, A. Georg, Electrochim. Acta 46 (2001) 3457–3466.